

4. J. L. Ord and F. C. Ho, *This Journal*, **118**, 46 (1971).
5. K. J. Vetter and J. W. Schultz, *J. Electroanal. Chem.*, **34**, 141 (1972).
6. A. Damjanovic and A. T. Ward, "International Review of Science, Physical Chemistry," Series II, p. 103, Butterworths, London (1976).
7. N. Cabrera and N. F. Mott, *Rep. Prog. Phys.*, **12**, 163 (1949).
8. J. O'M. Bockris and A.K.M.S. Huq, *Proc. Roy. Soc.*, **A237**, 271 (1956).
9. A. Damjanovic, A. T. Ward, and M. O'Jea, *This Journal*, **121**, 1186 (1974).
10. J. W. Schultz and K. J. Vetter, *Electrochim. Acta*, **18**, 889 (1973).
11. S. W. Feldberg, C. G. Enke, and C. E. Bricker, *This Journal*, **110**, 826 (1963).
12. K. J. Vetter and J. W. Schultz, *J. Electroanal. Chem.*, **34**, 131 (1972).
13. L. B. Harris and A. Damjanovic, *This Journal*, **122**, 593 (1975).
14. A. C. Makrides, *ibid.*, **113**, 1158 (1966).
15. R. W. Sirohi and M. A. Genshaw, *ibid.*, **116**, 910 (1969).
16. S. H. Kim, W. Paik, and J. O'M. Bockris, *Surf. Sci.*, **33**, 617 (1972).
17. A. K. N. Reddy, M. A. Genshaw, and J. O'M. Bockris, *J. Chem. Phys.*, **148**, 671 (1968).
18. W. Visscher, *Optic*, **26**, 407 (1967).
19. R. Parsons and W. Visscher, *J. Electroanal. Chem.*, **36**, 329 (1972).
20. H. A. Laitinen and C. G. Enke, *This Journal*, **107**, 773 (1960).
21. S. Gilman, *Electroanal. Chem.*, **2**, 111 (1967).
22. W. Visscher and M. Blijlevens, *Electrochim. Acta*, **19**, 387 (1974).
23. N. Sato and M. Cohen, *This Journal*, **111**, 512 (1964).
24. J. O'M. Bockris, M. Genshaw, V. Brusic, and H. Wroblowa, *Electrochim. Acta*, **16**, 1859 (1971).
25. H. Wroblowa, V. Brusic, and J. Bockris, *J. Phys. Chem.*, **75**, 2823 (1971).
26. A. Damjanovic and B. Jovanovic, *This Journal*, **123**, 374 (1976).

Influence of Substrate Structure on Electroless Gold Deposition

R. Sard* and B. C. Wonsiewicz

Bell Laboratories, Murray Hill, New Jersey 07974

ABSTRACT

The electroless gold process invented by Okinaka is capable of producing high quality gold conductors by direct deposition onto catalytic regions of a substrate. This study shows that the crystallographic orientation of the metal substrates onto which electroless gold is plated may have a profound effect on the process kinetics and the structure of the deposits. On single crystal copper substrates, the initial plating rate can vary by an order of magnitude with $\{111\} \gg \{100\} > \{110\}$. TEM studies show that the initial growth is epitaxial and accompanied by profuse microtwinning. X-ray pole figure results clearly show that the transition from slow initial plating on $\{100\}$ and $\{110\}$ to a much faster rate equivalent to that of the $\{111\}$ surfaces is due to the formation of a $\langle 111 \rangle$ preferred orientation which occurs due to complex multiple twinning processes. Experiments with a variety of technologically relevant polycrystalline substrates are in general agreement with the single crystal results. The substrate effects identified in this work as being important for the electroless gold plating process are believed to be applicable to other catalytic systems for metal deposition.

In 1969, Okinaka discovered a plating process capable of autocatalytic gold deposition which is therefore called electroless gold (1, 2). It is suitable for a number of electronic applications and has recently been applied to the formation of beam leads on integrated circuits (3). These applications have utilized the unique attribute of selective gold deposition at catalytic regions of a substrate. Substrates capable of catalyzing the electroless gold reaction include Pd, Pt, Cu, and other noble metals (4). The gold is only applied where needed, therefore, raw materials are saved and gold does not have to be etched away. Moreover, process steps can be eliminated resulting in further economies.

The deposition conditions profoundly influence the structure of the plated film and the plating rate. In a study which examined a wide range of plating variables, Sard identified two distinct growth morphologies, a lateral or layer type and an outward or particle type (5). The more three dimensional morphology, outward growth, is favored by several factors which increase deposition rate; namely, decreasing gold concentration, increasing reducing agent concentration, and increasing temperature. Agitation is an exception; increasing agitation increases the deposition rate but favors lateral growth.

* Electrochemical Society Active Member.

Key words: texture, structure, gold plating, catalysis.

Sard also concluded that the orientation of the substrate was important in determining the orientation of the plated film. The initial stages of growth (~ 10 nm) on single crystal substrates were epitaxial; that is, the orientation of the film reproduced the orientation of the substrate. Preliminary observations indicated that the plating rate was greatest for $\{111\}$ surfaces. When polycrystalline substrates were used, the orientation of thicker ($1 \mu\text{m}$) films was similar to the substrate, as measured by the ratio of peak intensities in an x-ray diffractometer.

Oriented growth has been commonly observed in thin films (6), especially those grown by vacuum deposition or electroplating. Under special conditions epitaxial growth occurs; more generally, the deposit has a low index crystallographic direction (the fiber axis) oriented perpendicular to the plane of the sheet, but is rotationally symmetric in the plane of the sheet. Such textures are called fiber textures, by analogy with a bundle of fibers arranged with their axes all pointing in the same direction. Under certain conditions, the fiber axis in deposited films can be tipped away from the film normal, usually toward the direction of greatest mass flux.

In view of the link between substrate orientation, plating rate, and orientation for the electroless gold system, a more detailed investigation was carried out.

A key improvement over previous studies was the use of x-ray pole figures to characterize the orientation distribution of the deposits. Pole figure determination is normally so tedious and time consuming as to rule it out for studying a large number of samples. However the use of a computer-aided system reduced the labor required to construct a pole figure from about 3 hr to 15 min (7).

The structure of films was studied at several stages of growth on single crystals and on several important polycrystalline substrates using the pole figure method. Additional data on the initial stages of growth were obtained by transmission electron microscopy (TEM), and scanning electron microscopy (SEM) was used to study the morphology of thick deposits. This approach has provided information relevant to some of the practical and fundamental aspects of electroless gold deposition. Some of our findings are undoubtedly applicable to other catalytic processes at solid/liquid interfaces.

Experimental Details

Single crystal substrates.—A copper single crystal 1.5 cm in diameter was grown by the Bridgeman method. Several thin slices 1 mm thick were spark cut parallel to each of the low index planes: {111}, {100}, and {110}. The orientation of the cut surfaces was within about 1° of the true planes.

Surface damage was removed by mechanical polishing followed by a chemical bright dip in an aqueous solution of 40% H₂SO₄, 20% HNO₃, and 0.1% HCl and electropolishing in 50% H₃PO₄ solution. After gold plating and the completion of measurements, the crystals were recycled by dissolving the gold in an iodide solution (8), rinsing in methanol, and water, then repeating the bright dip and electropolish procedures. After about 4 such cycles the crystals showed signs of increased surface roughness and had to be repolished mechanically. This changing surface roughness was probably responsible for some minor variations noted in the plating rate and microstructure on different regions of the samples and from run to run; however these effects were judged to be of second order importance and are not considered further.

Polycrystalline substrates.—A number of experiments were conducted using polycrystalline samples of two different types: (i) evaporated noble metal films (Au and Pd) on titanium-coated sapphire and glass, and (ii) copper metal sheets. A more detailed description of these materials and their preparation history is given together with the results below.

Electroless deposition.—For most experiments, electroless deposition was carried out using the solution formulation which was previously found to give the layer-type growth: KAu(CN)₂, 0.02M; KBH₄, 0.4M; KOH, 0.2M; and KCN, 0.2M. Unless otherwise specified, experiments were performed at 75° ± 0.5°C using a PTFE holder to maintain the substrates in cylindrical geometry. The agitation conditions were changed by introducing a glass stirrer with flattened blade coupled to an external motor rotating at 3000 rpm. A few experiments were also performed using a carousel arrangement in which the substrates rotated at about 150 rpm on a 2 in. diameter PTFE wheel. An alternate solution, formulated with 0.005M KAu(CN)₂, was also used for some experiments with forced agitation. This system was known to plate at a faster rate, due to its more negative deposition potential (9).

Film thicknesses were determined by the beta backscatter method using a promethium source and NBS calibration standards for the case of the bulk single crystal and polycrystalline Cu substrates. Although the absolute accuracy of these measurements is approximately ±5%, the results were checked against the weight gain method for sheet substrates and found to agree within 1-2%. The latter method was used for all thin film substrates. The plating rate was calculated by dividing the change in thickness averaged over the

sampling area by the plating time, based on the assumption of uniform deposits with the density of bulk gold.

Structure determination.—The crystallographic orientation distribution was determined by the standard pole figure technique (10) using Ni filtered Cu K_α radiation and the (111) Bragg reflection. A block diagram of the system is shown in Fig. 1. An automatic pole figure goniometer (either Siemens or Norelco) was used to rotate the specimen along a predetermined scanning geometry. X-ray intensity was recorded on punched paper tape using an Ortec digital ratemeter and printout control and a Model 35 Teletype. Specimen identification and values for constructing the intensity contours were entered directly on the paper tape. The tape, together with a group of Fortran IV programs served as input to a Honeywell H-6000 computer which generated the final drawings on a Xerox LDX graphics device. The present computer charges are about three dollars for a finished pole figure. The programs are capable of making corrections for background and absorption and will smooth data if necessary. Generally, no corrections were necessary in this study. The experimental techniques used gave good results for gold deposits in excess of 0.2 μm thick.

Microstructure results were obtained using the standard methods of interference contrast (Normarski) optical microscopy and scanning and transmission electron microscopy.

Results and Discussion

Single crystal substrates.—A typical set of results showing the effect of orientation on plating thickness as a function of time is illustrated in Fig. 2. The curves are drawn through averaged experimental points taken by removing the substrates periodically from a solution agitated with strong forced convection. The experimental points shown at the right edge of Fig. 2 were obtained by plating a similar set of substrates without forced convection. These data show clearly that the initial rate of gold plating, i.e., the initial slope, is highly orientation dependent with {111} > {100} > {110}, regardless of the transport conditions. By comparing the slopes over the interval 5-10 min and normalizing to {111}, one obtains relative rates for the three orientations of approximately 1 > 0.25 > 0.10. The interval from 0-5 min is complicated by the galvanic displacement effect which occurs in the first 10 nm of film growth. It is also evident from the curves that after 20 min, the rates are nearly the same

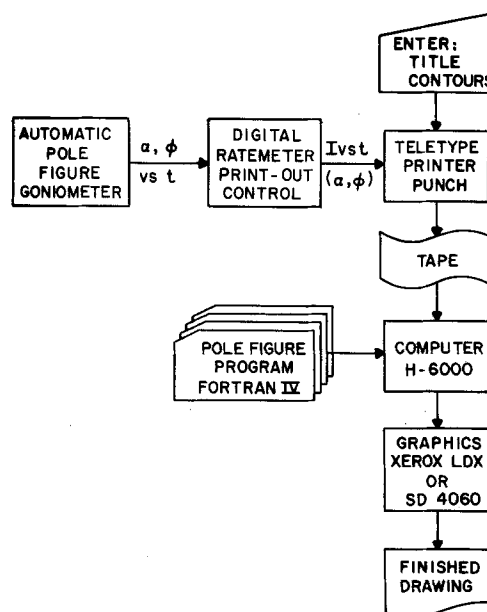


Fig. 1. Schematic of instrumentation used to obtain pole figures

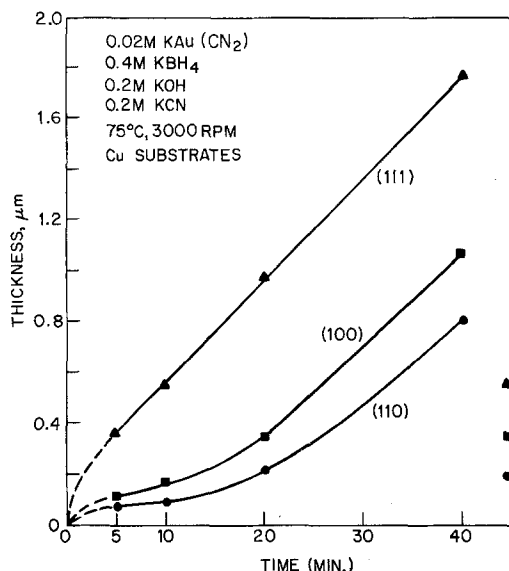


Fig. 2. Effect of orientation on electroless gold thickness vs. time of deposition.

on all three substrates, indicating a transition to steady-state conditions determined by the plating conditions. By following the changes in structure of such deposits, considerable insight was gained as to the physical aspects of the deposition mechanisms which govern this system.

The microstructures formed during the initial portion of the process, *i.e.*, the first 5 min or so, can be studied conveniently by transmission electron microscopy after chemical removal from the substrate (11). Figures 3a, 4a, and 5a illustrate the typical features evident in bright field images of Au deposits stripped from {111}, {100}, and {110} substrates, respectively, and their corresponding selected-area diffraction patterns are given in Fig. 3b, 4b, and 5b.

As the diffraction patterns show, the films at the earliest stages reproduce the substrate orientation, *i.e.*, the growth is epitaxial. This is apparently due to the displacement process as discussed previously (11). Small, parallel-sided features are visible in the micrographs; they are planar defects, small volumes of material which bear a twin orientation relationship with the matrix. In Fig. 3b, the six interior spots in hexagonal array are due to diffraction at the boundaries where twinning occurs. This result is similar to that for electroplated gold on copper (12). Similar microtwins have been observed in epitaxial evaporated films and the resulting twin-matrix structure is often called "double positioning" (13-15). The satellite reflections adjacent to the {100} reflections in Fig. 4b arise from double diffraction at the twin boundaries. This fact was confirmed by TEM dark field studies, *e.g.*, using the matrix and satellite spots encircled. The substructure evident in Fig. 3-5a is due primarily to the high density of twin faults which formed in the gold deposits.

The fact that these twins are due to deposition and not to deformation upon stripping the foils from the substrates was confirmed by the pole figures which were obtained with the deposits in place on the substrates.

Pole figures taken at the initial stages of film growth show quite clearly the epitaxial nature of the orientation as well as a weaker twin orientation. As the plating proceeds, the orientation distribution becomes more complex; the twin orientations with surface normals near $\langle 111 \rangle$ grow in volume most quickly.

Pole figures corresponding to a later stage of plating show a very intricate structure. The simplest structure is found on the fast plating {111} substrate. In the pole figure, Fig. 6a, the solid triangles locate the {111} substrate orientation and the open triangles locate the

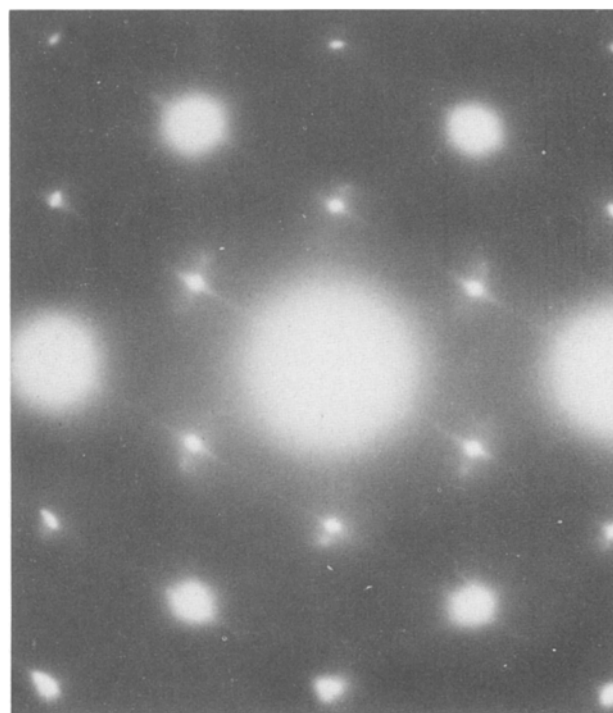
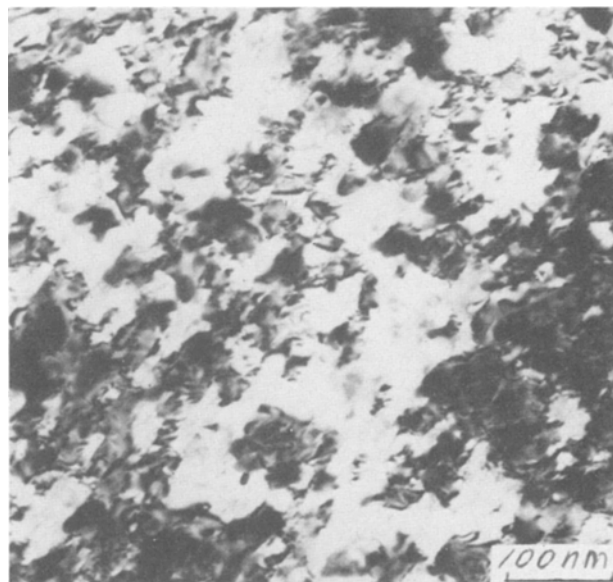


Fig. 3. TEM results for thin gold deposit on {111} substrate. (a, top) Bright-field image, original magnification 120,000 \times . (b, bottom) Selected-area diffraction pattern.

twin orientation. The twinned material has mirror symmetry with the original matrix. This matrix-twin relationship is equivalent to the "double-positioning" structure evident in the early stages of film growth shown in Fig. 3.

The more complex structure evident in Fig. 6b is found in films plated on the {100} substrate. The pseudo-twelvefold symmetry apparent in the pole figure also arises from twinning. In the original epitaxial deposit, there are four $\langle 111 \rangle$ poles symmetrically oriented as indicated by the four half-filled squares in Fig. 6b. Twinning on one of the {111} planes will produce the orientation shown as open squares labeled A(1) through A(4). Twinning on the other three original {111} planes produces the rest of the poles shown by open squares. Note that the twinning places four $\langle 111 \rangle$ directions within 15.8° of the surface normal. Nevertheless the actual intensity recorded in Fig.

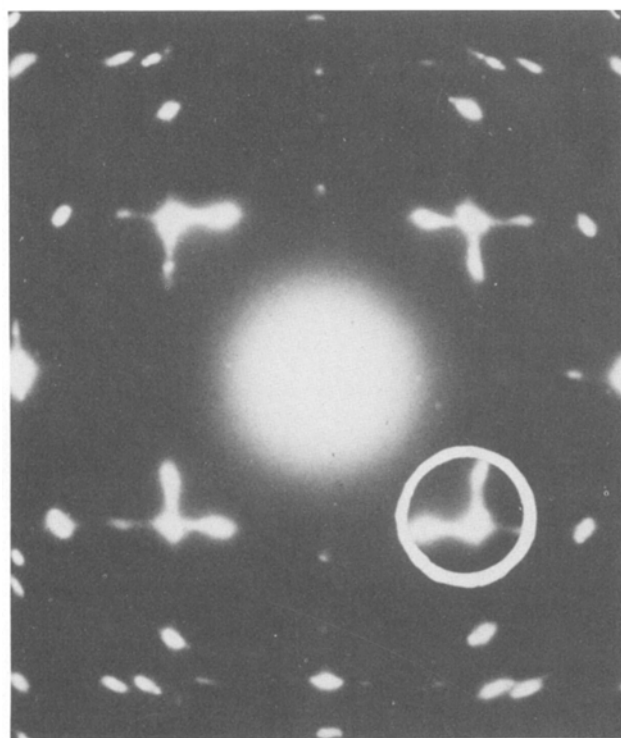


Fig. 4. TEM results for thin gold deposit on $\{100\}$ substrate. (a, top) Bright-field image, original magnification $110,000\times$. (b, bottom) Selected-area diffraction pattern.

6a is greatest at the surface normal rather than 15.8° away. This indicates a rotation during growth to a final $\{111\}$ film orientation. As can be seen in Fig. 6b, little intensity remains in the region of the original $\{100\}$ orientation and the transition to the final $\{111\}$ orientation is highly developed.

The films plated on the $\{110\}$ copper substrate have a still more complex orientation. The original epitaxial orientation is indicated on the pole figure shown in Fig. 6c by the lens symbol. Note that there are twenty intensity maxima in addition to the two located by the original epitaxial orientation. All of them can be precisely located by twinning reorientations. The first

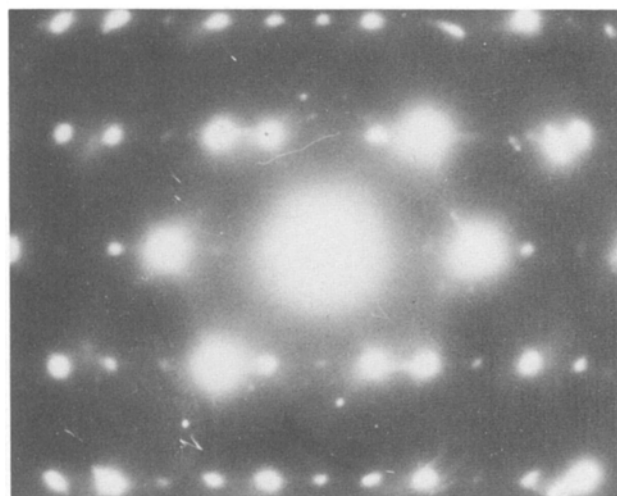
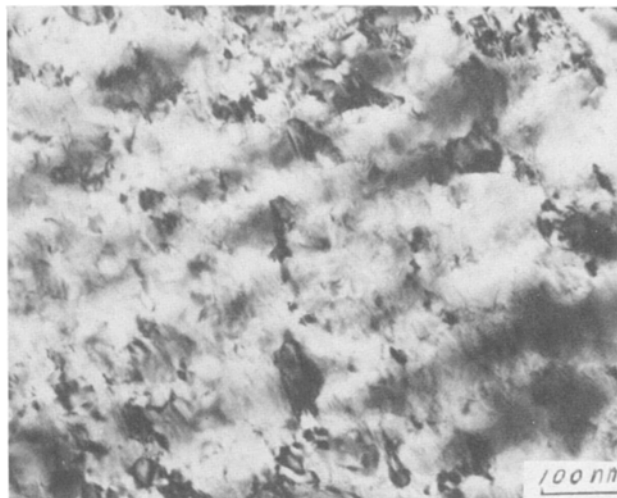


Fig. 5. TEM results for thin gold deposit on $\{110\}$ substrate. (a, top) Bright-field image, original magnification $120,000\times$. (b, bottom) Selected-area diffraction pattern.

group of orientations indicated by the squares in Fig. 6c were produced by twinning on the two $\{111\}$ planes visible in the pole figure; the new orientation locates the film normal about 19.5° away from $[001]$. The second group of orientations indicated by triangles is obtained by retwinning of the previous orientation, the squares. The twin plane normal is designated by an overlapping square and triangle. After twinning first on the square and then on the triangle, the new orientation of the doubly twinned material is within 5° of the fast growing $\{111\}$ orientation. The remaining group of orientations designated by the circles can be produced by twinning first on the triangles and then retwinning on the plane indicated by the overlapping circle and triangle. This doubly twinned volume is oriented about 25° from $\langle 111 \rangle$, midway between $\langle 112 \rangle$ and $\langle 113 \rangle$. The combination of primary twinning followed by two different types of secondary twinning can explain all the maxima observed in Fig. 6c.

A generalization of the single crystal results is that the substrate orientation is reproduced in the film and that additional orientations are generated by $\{111\}$ twinning. If the twinning or retwinning process places a $\langle 111 \rangle$ direction in the vicinity of the film normal, a transition to a $\{111\}$ film orientation begins. Agitation did little to modify these observations, except to produce slightly asymmetrical pole figures. When strong convection was present, orientations with $\langle 111 \rangle$ directions inclined toward the direction of fluid flow were the most intense. This is in agreement with the observations of film growth from the vapor; namely

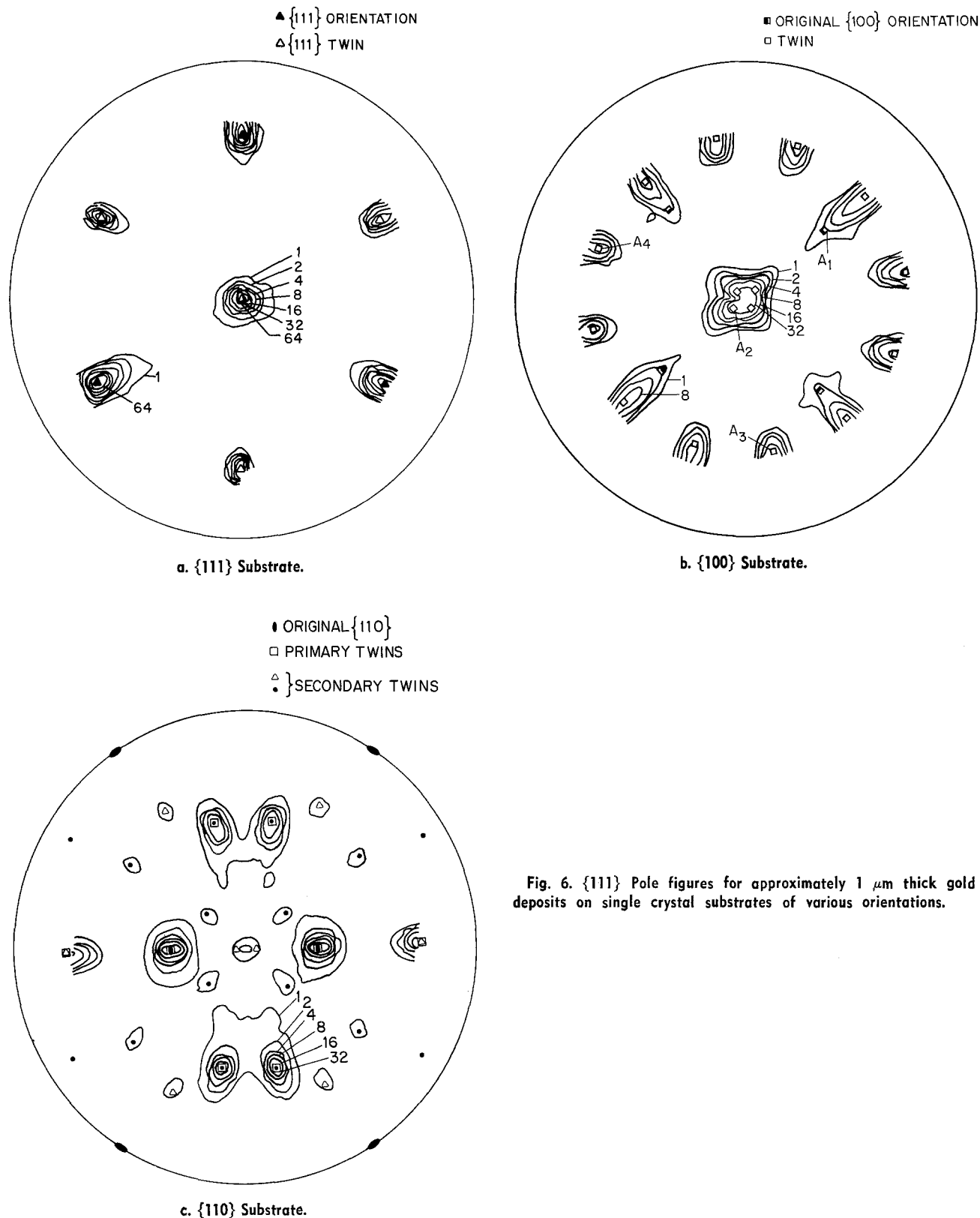


Fig. 6. {111} Pole figures for approximately $1 \mu\text{m}$ thick gold deposits on single crystal substrates of various orientations.

that the $\langle 111 \rangle$ direction is inclined toward the direction of greatest mass flux (6).

An interesting correlation exists between the change in plating rate, shown in Fig. 2, and the change in film orientation due to twinning. Once the various complex twinning mechanisms operative for the {100} and {110} substrates have taken place, the deposits all tend toward the $\langle 111 \rangle$ preferred orientation and the rate of deposition becomes independent of substrate. At this point, the kinetics of the electroless gold reaction have reached steady state and are controlled by the deposition conditions and the mixed-electrode potential (9).

The catalysis literature contains numerous papers dealing with the effect of crystal orientation on the kinetics of gas phase reactions (16, 17), and the role of structural factors in electrocatalysis (18). Crystallographic orientation is the most important structural factor controlling the catalytic activity of platinum surfaces in studies of hydrogen evolution and the anodic oxidation of methanol (18). The rates of these reactions were greatest on the {111} face by up to an order of magnitude, as compared to other crystal faces with lower atomic packing density. Our results for the electroless gold system are in good agreement with these findings, as has been pointed out by Okinaka (9)

who noted that the chemisorption of reacting species is an important feature of catalytic processes. Other results from electrocrystallization studies have shown that exchange current densities for the electrodeposition of copper on copper single crystals increases by a factor of five on going from $\{111\}$ to $\{100\}$ to $\{110\}$. This means that the rate of deposition at constant overpotential increases in the order $\{110\} > \{100\} > \{111\}$ (19). The electroless gold results (Fig. 2) are exactly opposite. Thus, from the standpoint of the deposition mechanism, the electroless gold has more in common with the electrocatalysis of platinum than the electrocrystallization of copper. One aspect of the electroless gold process not studied in this work but discussed elsewhere (9), is that the anodic reaction may be rate controlling.

Examination of the surfaces of the electroless gold deposits by optical microscopy and SEM also showed that the substrate orientation strongly affects the growth morphology, consistent with the established literature on electrocrystallization studies (20). Normarski optical microscopy revealed that the deposit on the $\{111\}$ substrate consisted of 200-400 μm features that were similar to previously reported structures for thick copper deposits on $\{111\}$ (21). The other two substrate orientations yielded surfaces with much finer features that could not be resolved optically. Representative SEM results are shown in Fig. 7a-c for the $\{111\}$, $\{100\}$, and $\{110\}$ substrates, respectively. Because of the large features on the $\{111\}$ surface, there is relatively little structure visible at high magnification unless one looks near the edges of the features as in Fig. 7a. The appearance of the surface on the $\{100\}$ substrate (Fig. 7b) is quite similar to the smooth faceted structure which is commonly observed for technological deposits on polycrystalline substrates under these plating conditions (4). The deposits on the $\{110\}$ substrate have an irregular microstructure with numerous fine features ($\sim 0.2 \mu\text{m}$) as well as larger ones ($> 2 \mu\text{m}$). These results suggest that the process of lateral growth occurs most readily on $\{111\}$ substrates which is in agreement with recent findings for gold electrodeposits (22). Consideration of these data together with the plating rates (Fig. 2) and pole figures (Fig. 6) indicates that the twinning processes, the microstructure, and the nonuniform initial plating rates are interrelated.

Polycrystalline substrates.—Evaporated films.—Two sets of experiments were carried out using evaporated film substrates and the standard plating solution. In the first set, either Pd or Au films, 80 nm thick, were evaporated at 1.5 nm/sec using an e-beam system at 2×10^{-7} Torr onto a 30 nm thick layer of Ti which was freshly deposited onto clean, polished sapphire surfaces 9 mm \times 2.0 cm in size. Three samples of each type of film were mounted in a PTFE holder and plated simultaneously either in still solutions or with vigorous stirring using a rod at 3000 rpm. The effects of agitation on plating rate have been discussed in detail elsewhere (4). The rate of deposition was 40% greater on the Au substrate than on the Pd substrate if the solution was agitated. Without agitation the difference was 20%. Since the difference in plating rate was suspected to be due to a difference in the structure of the substrates, the structure of both the substrates and deposits was studied in some detail. Pole figures for the deposits on the gold substrates showed a very strong $\langle 111 \rangle$ fiber feature which was also quite strong in the substrate films; whereas, the gold deposits on Pd substrates showed a weaker $\langle 111 \rangle$ fiber texture as did the substrates which were much more randomly oriented. Since the $\langle 111 \rangle$ orientation is known to plate at a fast rate, Fig. 2, the difference in plating rate is probably due in part to the difference in orientation. Further examination of the substrates by TEM showed that the Pd films were uniformly fine grained (~ 10 nm) and the Au films

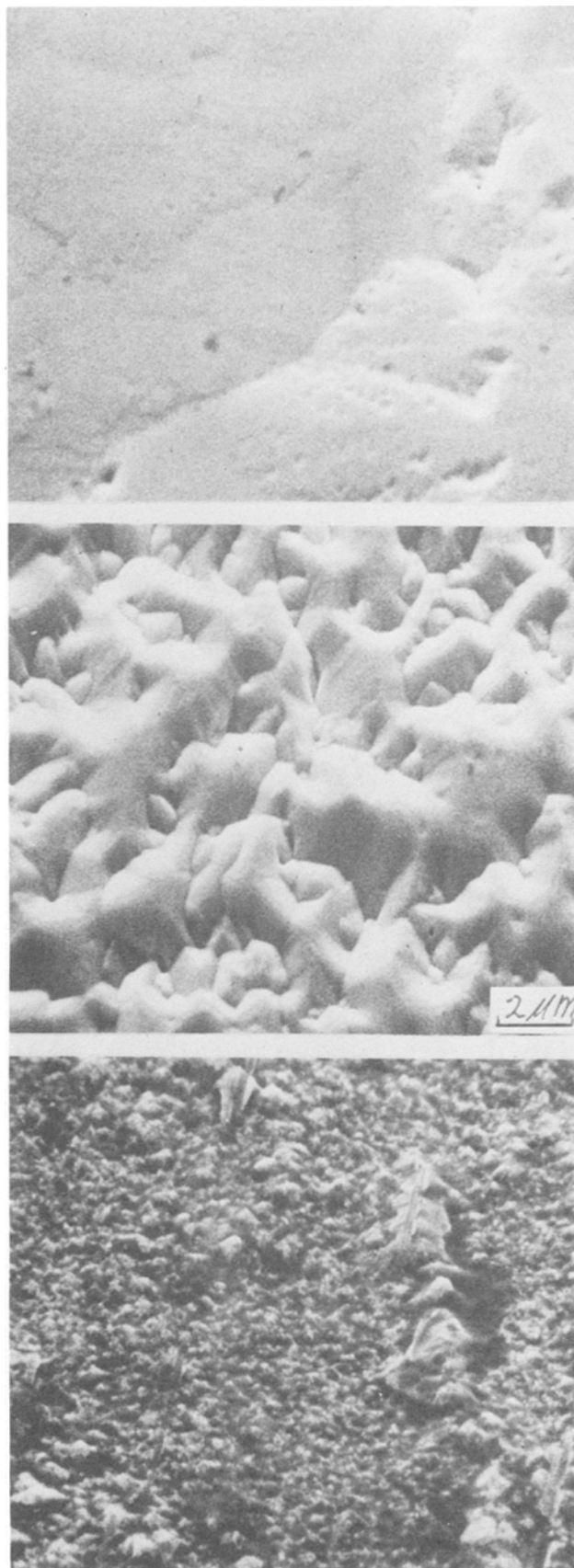


Fig. 7. SEM results showing surfaces of thick gold films on single crystal substrates, original magnification 5000 \times . (a, top) $\{111\}$ Substrate. (b, center) $\{100\}$ Substrate. (c, bottom) $\{110\}$ Substrate.

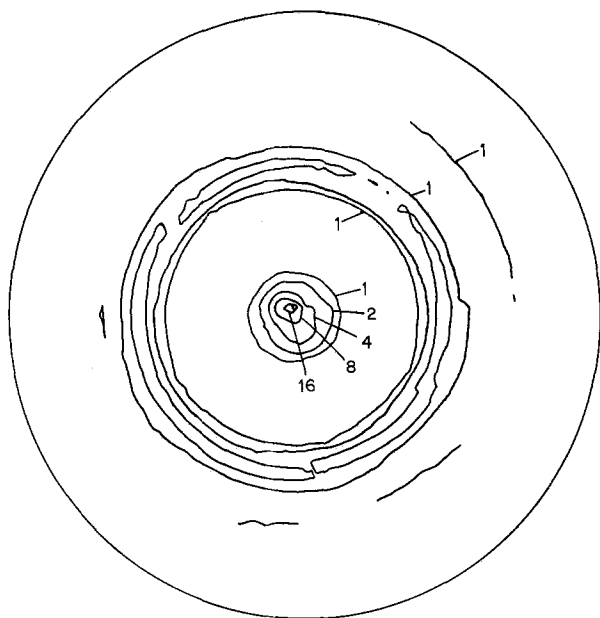
were more heterogeneous with many grains > 100 nm in size.

In a second series of experiments Au/Ti/glass substrates were evaporated at higher pressure ($\sim 2 \times 10^{-5}$ Torr). These substrates had a complex texture. The fiber axis was tilted away from the sheet normal toward the direction of mass flux during evaporation. The texture consisted of a strong $\langle 111 \rangle$ component combined with a weaker $\langle 100 \rangle$ component. The substrates were plated in the standard solution with different amounts of agitation. Figure 8a gives the pole figure for a 2 μm thick deposit plated without agitation at the normal rate of 0.7 $\mu\text{m/hr}$. The plated film reproduced the orientation of the substrate. The more complex pole figure in Fig. 8b corresponds to a deposit plated in the same bath to the same thickness but with carousel stirring at a velocity of 0.46 m/sec which produces a threefold increase in plating rate (4). These conditions yield a $\langle 111 \rangle$ fiber texture with a strong $\langle 311 \rangle$ component as seen in Fig. 8b.

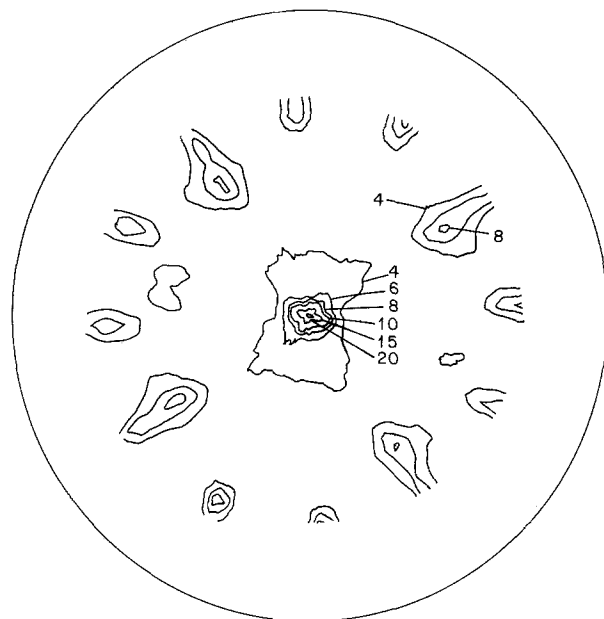
In both of these sets of experiments with evaporated noble metal film substrates it was found that the deposits were formed epitaxially and that the $\langle 111 \rangle$

orientation of the substrates was maintained for deposits $< 2 \mu\text{m}$ in thickness. Subtle but real effects due to substrate grain size and the strength or degree of the $\langle 111 \rangle$ texture were observed.

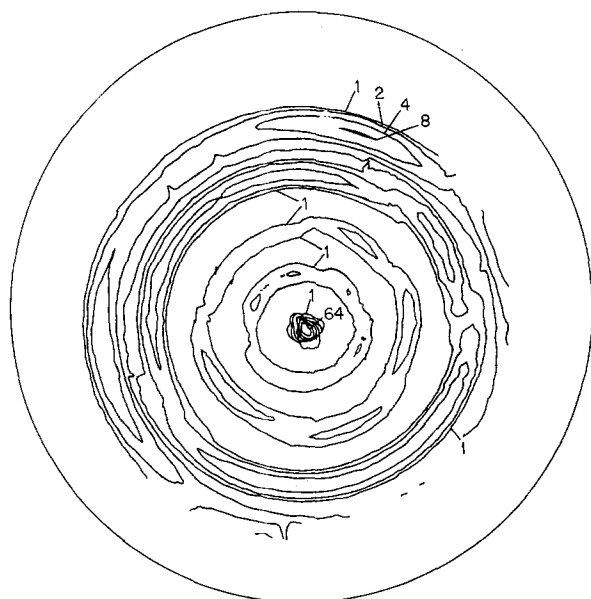
Rolled sheet metal.—In an initial set of experiments, two lots of nominally identical commercial copper foil plated at substantially different rates under the same conditions (23). One batch of material gave the normal plating rate (1.5 $\mu\text{m/hr}$) and the other showed a surprising twofold increase in rate which was maintained to a thickness of $> 5 \mu\text{m}$. Pole figures for both substrates showed them both to be qualitatively the same, with cube textures as expected. Figure 9a shows the pole figure for the deposit with the normal plating rate. Here we see the characteristic epitaxial growth of the cube texture and the transition to $\{111\}$ by the multiple twinning mechanism which has already been discussed for the case of the $\{100\}$ single crystal substrate, Fig. 6b. Figure 9b shows that the anomalously fast plating deposit remained in the cube orientation.



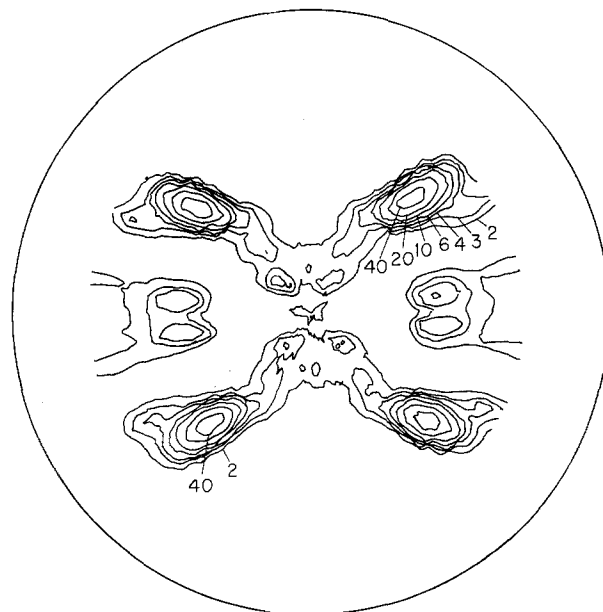
a. No agitation, plating rate 0.7 $\mu\text{m/hr}$.



a. Normal plating rate 1.5 $\mu\text{m/hr}$.



b. Agitation at 2750 cm/min, plating rate 2.1 $\mu\text{m/hr}$.



b. Anomalous plating rate 3.0 $\mu\text{m/hr}$.

Fig. 8. $\{111\}$ Pole figures for 2 μm thick gold deposits on evaporated gold thin film substrates.

Fig. 9. $\{111\}$ Pole figures for thick gold deposits on copper sheet substrates of commercial material.

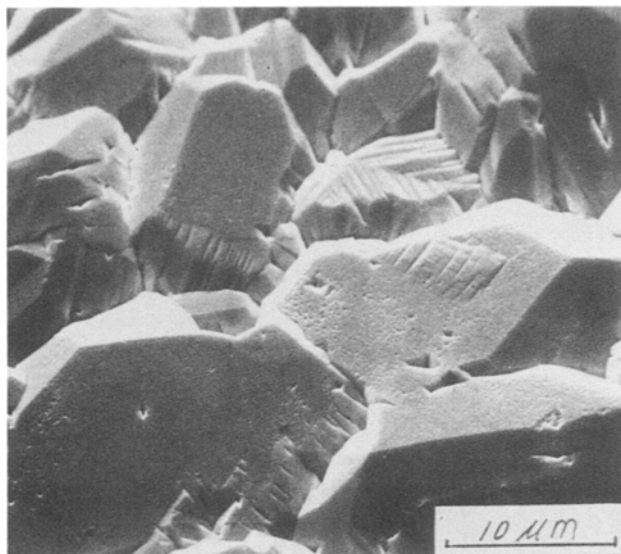


Fig. 10. Surface structure corresponding to Fig. 9b, original magnification $2500\times$.

The microstructure of this deposit observed in the SEM was also unusual and is shown in Fig. 10. Here we see a large, faceted grain structure with smooth features $\sim 20\ \mu\text{m}$ across whereas the deposits plated at the normal rate showed a considerably finer microstructure with background features $1\text{--}2\ \mu\text{m}$ in size and some larger, nodular features.

A SEM examination of etched samples of the two substrates indicated some qualitative differences such as the grain size and shape but did not permit us to explain the anomalously high plating rate. One possibility is that an impurity species, which may have dissolved from the surface region of the fast copper substrate during the initial displacement process, somehow altered the growth process by preventing the twinning mechanism from occurring. However, in this case we would expect the rate to be slow as one finds with $\{100\}$ single crystals; but this is not the case for this material by at least an order of magnitude.

Additional experiments were conducted in an attempt to shed some light on the above result and see whether or not it could be reproduced using other copper sheet substrates. To do this, we started with bulk OFHC Cu and prepared sheet samples, 0.010 in. thick, by cold rolling to a 92% reduction. The pole figure in Fig. 11 indicates that this texture is copied by the electroless gold deposit, which in this case was $1.5\ \mu\text{m}$ thick and plated at the normal rate. Deposits plated on annealed substrates from the same material (300°C , 1 hr) showed a similar plating rate and the expected structure for the case of cube-texture substrates, i.e., identical to Fig. 9a. This set of experiments included other sheet substrates (Au and phosphor bronze) and plating runs at temperatures both 10°C above and below nominal. In no case were we able to find any increase in the plating rate, comparable to that observed with the "fast copper."

Summary and Conclusions

The results of this study show that the structure of metal substrates onto which electroless gold deposits are plated may have a profound effect on the process kinetics and the structure of the deposits. On single crystal copper substrates, the initial plating rate can vary by an order of magnitude with $\{111\} \gg \{100\} > \{110\}$. In all three cases twinning is observed during the initial stages of growth ($\sim 0.1\ \mu\text{m}$). The TEM results show twin fault densities $> 10^{+11}/\text{cm}^2$. X-Ray pole figures for thick deposits provide additional evidence for the importance of twinning in this deposition process. In particular, the pole figure results indicate that multiple twinning processes are responsible for

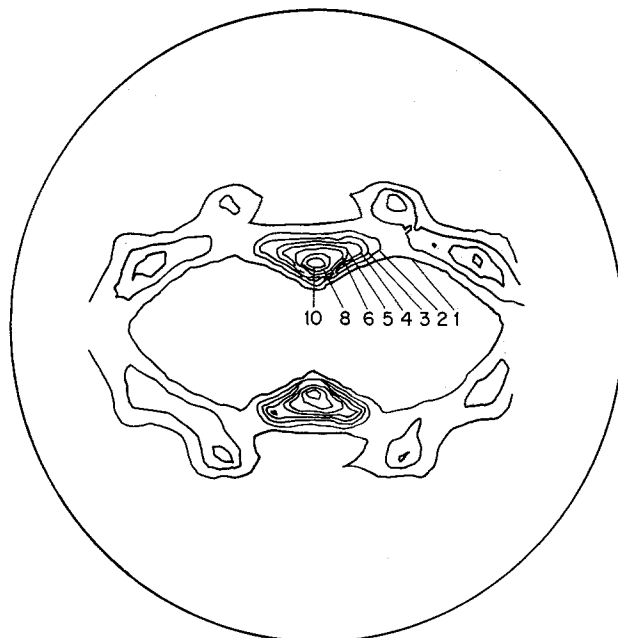


Fig. 11. $\{111\}$ Pole figure of $1.5\ \mu\text{m}$ thick gold deposit on cold-rolled OFHC copper sheet.

the transition from the slow initial plating rates on the $\{100\}$ and $\{110\}$ substrates to the faster rate typical of the $\langle 111 \rangle$ preferred orientation.

Electroless gold deposits on evaporated noble metal film substrates exhibit a $\langle 111 \rangle$ fiber axis which represents a continuation of the substrate texture. A somewhat lower rate of deposition is observed for Pd substrates relative to that on Au films. The magnitude of this effect is about 20% without forced convection and about 40% when the plating solution is stirred vigorously. The somewhat lower plating rate on Pd is apparently due to the fact that these substrate surfaces are comprised of much smaller grains ($\sim 10\ \text{nm}$) that are more randomly oriented than the Au films.

Experiments with polycrystalline Cu sheet substrates are in general agreement with the single crystal results except for one particular batch of commercial material onto which deposits with an unusually large grained microstructure were formed at an anomalously fast plating rate. This result could not be reproduced with laboratory-prepared sheet substrates.

We conclude by noting that the substrate effects identified in this work as being important for the electroless gold plating process are likely to be applicable to other catalytic systems for metal deposition. This would appear therefore to be a fruitful area for further work.

Acknowledgment

The authors wish to thank Y. Okinaka for his help and advice throughout this study.

Manuscript submitted Aug. 12, 1975; revised manuscript received May 20, 1976.

Any discussion of this paper will appear in a Discussion Section to be published in the June 1977 JOURNAL. All discussions for the June 1977 Discussion Section should be submitted by Feb. 1, 1977.

Publication costs of this article were assisted by Bell Laboratories.

REFERENCES

1. Y. Okinaka, *Plating*, **57**, 914 (1970).
2. Y. Okinaka, in "Gold Plating Technology," F. H. Reid and W. Goldie, Editors, chap. 11, Electrochemical Publications, Ltd., Scotland (1974).
3. R. Sard, Y. Okinaka, and H. A. Waggner, *This Journal*, **121**, 62 (1974).
4. Y. Okinaka, R. Sard, W. H. Craft, and C. Wolowoduik, *ibid.*, **121**, 56 (1974).

5. R. Sard, Abstract 134, p. 220, The Electrochemical Society Extended Abstracts, Fall Meeting, Cleveland, Ohio, Oct. 3-7, 1971.
6. K. L. Chopra, "Thin Film Phenomena," p. 220, McGraw-Hill Book Co, New York (1969).
7. B. C. Wonsiewicz, "Rapid Computer Plotting of Pole Figures," Bell Laboratories, Murray Hill, New Jersey (1972).
8. Handbook of Thin Film Technology, L. I. Maissel and R. Glang, Editors, pp. 7-37, McGraw-Hill Book Co., New York (1970).
9. Y. Okinaka, *This Journal*, **120**, 739 (1973).
10. C. S. Barrett and T. B. Massalski, "Structure of Metals," 3rd ed., pp. 193-222, McGraw-Hill Book Co. New York (1966).
11. R. Sard, *This Journal*, **117**, 1156 (1970).
12. E. R. Thompson and K. R. Lawless, *Electrochim. Acta*, **14**, 269 (1969).
13. D. W. Pashley and M. J. Stowell, *Philos. Mag.*, **8**, 1605 (1963).
14. D. W. Pashley, *Adv. Phys.*, **14**, 327 (1965).
15. R. D. Burbank and R. L. Heidenreich, *Philos. Mag.*, **8**, 651 (1963).
16. A. T. Gwathmey and R. E. Cunningham, *Adv. Catal.*, **10**, 57 (1958).
17. H. Jaeger, *J. Catal.*, **9**, 237 (1967).
18. V. S. Bagotzky, Yu. B. Vassiliev, and I. I. Pyshnograeva, *Electrochim. Acta*, **16**, 2141 (1971).
19. J. O'M. Bockris and A. K. N. Reddy, "Modern Electrochemistry," Vol. 2, p. 1215, Plenum Press, New York (1970).
20. See, e. g., R. Piontelli, G. Poli, and G. Serravalle, "Transactions of the Symposium on Electrode Processes," E. Yeager, Editor, p. 67, John Wiley & Sons, New York (1961).
21. U. Bertocci and C. Bertocci, *This Journal*, **118**, 1287 (1971).
22. R. J. Morrissey and A. M. Weisberg, *Trans. Inst. Met. Finishing*, **53**, 9 (1975).
23. Y. Okinaka, Private communication.

Electrodeposition of Cobalt Using an Insoluble Anode

G. R. Lakshminarayanan, E. S. Chen, J. C. Sadak, and F. K. Sautter

Benet Weapons Laboratory, Watervliet Arsenal, Watervliet, New York 12189

ABSTRACT

A method has been developed which permits the use of an insoluble anode to electrodeposit cobalt by the addition of a sufficient amount of an electrochemically active substance such as vanadium pentoxide to the cobalt sulfate plating solution. In the absence of such additions, formation of Co^{3+} ions and cobalt oxide (Co_2O_3) at the platinum anode results during plating. The effects of the addition of vanadium pentoxide on the electrode process during plating have been investigated through the analyses of various electrolysis products as a function of additive concentration and plating time. The results show that besides cobalt deposition, vanadium ions of lower oxidation state (V^{++} , V^{+++} , VO^{++}) are formed at the cathode and these ions seem to be responsible for the reduction and suppression of Co^{3+} ions and the oxide at the platinum anode. It has also been observed that the concentration of the added electrochemically active substance changed very little, indicating no incorporation of vanadium with the deposit during plating. The mechanical properties of the deposits prepared using an insoluble anode are compared with those obtained using a soluble anode.

The electrodeposition of cobalt, dispersion-hardened cobalt, and cobalt-based alloys has been the subject of investigation (1-6) at this laboratory for many years because of the potential application as protective coatings to improve the wear and erosion characteristics of the substrates. In conventional cobalt plating, soluble anodes are used to replenish the metal deposited at the cathode. In plating the inside of small bore tubes such as small caliber gun tubes, however, it would be necessary and also highly advantageous to use an insoluble anode since the dimensions of the anode would not change. However, the use of an insoluble anode like platinum in cobalt plating solutions leads to the formation of undesirable black cobalt oxide particles at the anode. They appear at the anode as a strongly adherent black coating or remain as suspended particles in the plating solution. The codeposition of these particles with the deposits has a detrimental effect on the structure and properties of the deposits. In order to suppress the undesirable reactions leading to the formation of cobalt oxide, other electrochemically active substances were introduced in the plating solution. It was hypothesized that the oxide formation could be suppressed if other reducible agents were present in the electrolyte. The additive should be such that it does not interfere with the normal plating process and has no detrimental effect on the properties of the deposit. Vanadium pentoxide was found to be a very

effective and suitable chemical in this regard. By undergoing reduction at the cathode and oxidation at the anode without being codeposited, this substance provides electrochemically active species during plating which suppress the oxide formation. This investigation deals with a study of the effects of addition of vanadium pentoxide to the cobalt sulfate plating solution on the electrodeposition of cobalt using a soluble or an insoluble (platinum) anode.

Experimental

Plating solutions and plating procedure.—All chemicals were of reagent grade quality and were used without further purification. A stock solution of cobalt sulfate (1.0M) was prepared and unless otherwise stated, 150 ml fresh solution was used for each experiment. Vanadium pentoxide (up to about 4.5 g/liter) was added to the plating solution. The dissolution of vanadium pentoxide was slow and it took up to 50-60 hr to dissolve 4.5 g/liter at 40°C and at pH 1.0. A regulated power supply was used as a power source. Cobalt or platinum anodes and stainless steel or brass cathodes (substrates) were used for plating. Cobalt plating was generally carried out at a current density of 5 A/dm², a temperature of 40°C, and at an initial pH 1.00.¹

¹ The low pH was used, in spite of reduced cathode efficiency, in order to obtain increased solubility of V_2O_5 and reduced formation of black oxide particles.

Key words: insoluble anode, electrochemically active substances, electrode process.